RSC Advances

ROYAL SOCIETY OF CHEMISTRY

www.rsc.org/advances

Journal Name

RSCPublishing

ARTICLE

Visual Monitoring of Laser Power and Spot Profile in Micron Region by a Single Chip of Zn Doped CdS Nanobelts

Cite this: DOI: 10.1039/x0xx00000x

Received ooth January 2012,
Accepted ooth January 2012

DOI: 10.1039/x0xx00000x

www.rsc.org/

Xiaoxu Wang, Wensheng Zhang, Guangli Song, Bingsuo Zou, Zhishuang Li, Shuai Guo, Jing Li, Qisong Li, Ruibin Liu*

On the basis of pumping-power-dependent emission property, the single-chip zinc doped cadmium sulfide nanobelts are developed to monitor the injected laser power and detect the profile of laser focal spot visually in micron region through the color changes. Utilizing doping zinc into cadmium sulfide nanobelts, band-edge emission with green color and deep-trap-state emission with red color are generated by injected laser beam pumping. The monotonic intensity-ratio changes of these two emission reflect the pumping power variations, so that the laser power and focus spot distribution are monitored quantitatively by the on-chip nanobelts. As utilized on-chip zinc doped cadmium sulfide nanobelts to detect the input laser power, more than two thousand cycles of pumping laser power increasing and decreasing periodically are applied on the nanomaterial chip, accompanied with the emission-color switching between yellow-color emission and green-color emission, which confirm that the zinc doped cadmium sulfide nanobelts are stable and effective. It visually perceives the change of laser power and detects the distribution profile of the laser spot. This optical ratiometric method based on nanostructures is quite different from the traditional detection mode by thermoelectric effect. Therefore, it has potential application as laser power monitor tools on optically integrated micro-circuit.

Introduction

Laser power detector has been widely studied and developed due to it is a critical tool for the experimental studies on optical properties. Generally, the traditional laser power meter utilizes the pyroelectric-type detectors or laser photodiode as a basic detect element. Using this method, the laser power intensity was transferred to voltage signal to get the laser power value precisely.[1, 2] It needs additional display module to show the power value except the detector. Moreover, for the thermoelectric effects, a complicated cooling part is required to dissipate the heat. Therefore, it is hard to obtain miniaturized and embedded optical power sensor with traditional material and route to satisfy the development of nanotechnology and nanodevice even though it is acritical component in the photonic integrated circuit.[3, 4] For photodiode type power detector，it is always used in low-power injection situation and, and generally need a filter together to avoid damage by input laser. Actually, until now, there is still no any power detector could give us a visual and intuitive perception of power value and distribution profile of input laser beam in micron region. In this paper, we firstly demonstrate a new way to detect the input laser power visually and intuitively based on nanobelt-integrated chip. Utilizing nanostructures as basic power monitor element, it guarantees the easy way to integrate with developed micro/nanodevice to build-up more complicated optical circuit with higher functionality.

Nanostructures of the Ⅱ-Ⅵ group semiconductor are one kind of advanced optical materials with excellent light-emitting and optoelectronic properties.[5, 6] Generally, doping metal impurities into II-VI group semiconductor always generate additional defect related energy levels, together with band-edge emission to form ratiometric photoluminescence (PL) intensity, which was developed to realize the optical ratiometric sensor.[7] In recent reports, wide-gap Ⅱ-Ⅵ nanocrystals doped with manganese ions (Mn^{2+}), exhibiting the optically ratiometric properties on the detection of the various local environmental changing, have attracted many attentions.[8, 9] The optical ratiometric method has been widely applied on the detection of excitation intensity,[10] temperature,[11] PH,[12] heavy metals in solutions[13] and toxic gas in mitochondria.[14] Optically ratiometric sensor shows resolvable luminescence from two different excited states. The light intensity is measured by the relative PL intensity ratio instead of absolute PL intensity,[7, 15] which will not induce thermal effects and the complicated cooling system could be ignored. It makes the device minimized and realized all-optical integrated circuit easily.[16, 17] Moreover, the analysis on intensity distribution of laser focus is important for some nonlinear optical phenomenon, such as two photon absorption and sub-wavelength spatial resolved excitation.[18, 19] However, up to date, few results on

nanostructure-related laser power monitor were mentioned, especially for the intensity distribution of laser focus in micron-region.

In this work, the single-chip zinc doped cadmium sulfide (Zn doped CdS) nanobelts were synthesized by a controllable chemical vapor deposition (CVD) method, which was used to detect the laser power and intensity distribution visually in micron region according to the power-dependent properties of two distinct emission bands at room temperature. Under a power-variable UV laser illumination, the ratio of these two distinct emission color will change relatively with different pumping power change. Therefore, the power distribution of laser focus spot can be shown directly by a real-color image in microsize region on the Zn doped CdS nanobelt chip. Moreover, the color tunable property of the on-chip Zn doped CdS nanobelts is extraordinarily stable with the laser power changing during an experimental period of 6-monthes. This new idea on laser power detector and profile measurement of pumping laser spot based on nanostructures provides more possible applications on visual laser power detection.

Experimental

The synthesis method of Zn doped CdS nanobelts is similar to the ever published CVD results.[20] The morphology, phase structure, and elemental valence state of Zn doped CdS nanobelts are characterized by a field-emission scanning electron microscope (SEM, Zeiss SUPRA 55), an x-ray diffractometer (XRD, RINT2200), a an X-ray photoelectron spectroscopy (XPS, Thermo Scientific), respectively.
In the experiments of laser power monitor and the intensity distribution analysis, a confocal PL microscopy was used with the spatial resolution 500 nm (Olympus BX51M, X50 objective lens, NA~0.46). Specially, the pumping laser power was fine-tuned by the driven voltage of diode laser (GaN diode laser ~405 nm).

Results and discussion

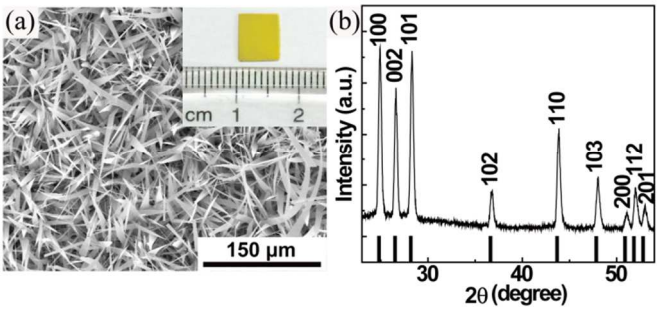

Fig. 1. (a)The SEM image of Zn doped CdS nanobelts. The inset is an image of on-chip Zn doped CdS nanobelts . (b) X-ray diffraction pattern of the single-chip Zn doped CdS nanobelts.

In this work, we designed the CdS nanobelts with ~2% of Zn dopant, which show a strong yellow color PL emission under proper excitation power. The SEM image exhibits the morphology of Zn doped CdS nanobelts is belt-like and uniform with ~20 μm base length and ~300 μm waist length, as shown in Fig. 1 (a). The inset in Fig. 1 (a) is an image of the single-chip of Zn doped CdS nanobelts with the size of 0.6cm*0.6cm. The XRD patterns of the on-chip Zn doped CdS nanobelts exhibit major peaks corresponding to diffraction lines of the structure of hexagonal wurtzite phase CdS (JCPDS Card No.41-1049), as shown in Fig. 1 (b). No distinct peaks of secondary phases and deviation shown in the XRD pattern confirm the good crystallinity of the nanobelts.

The full-range XPS spectrum exhibits that the as-prepared sample consists of the elements Cd, S and Zn, with no obvious impurities except the inevitable elements C and O, as shown in Fig. 2 (a). The Cd $3d^{2/5}$ peak at 404.6 eV (Fig. 2 (b)) and the Zn $2p^{3/2}$ peak at 1021.5 eV (Fig. 2 (d)) are consistent to the reported binding energies for Cd^{2+} and Zn^{2+}; the S $2p^{3/2}$ peak at 160.9 eV (Fig. 2 (c)) and the S $2p^{3/2}$ peak at 168.2 eV are consistent to the reported binding energies for S^{2-} and S^{6+}. The XPS analyze the surface element of the sample, so the existence of S^{6+} comes from the surface oxidation of the nanobelts. These characterizations demonstrated that the Zn doped CdS nanobelts were prepared with high quality.

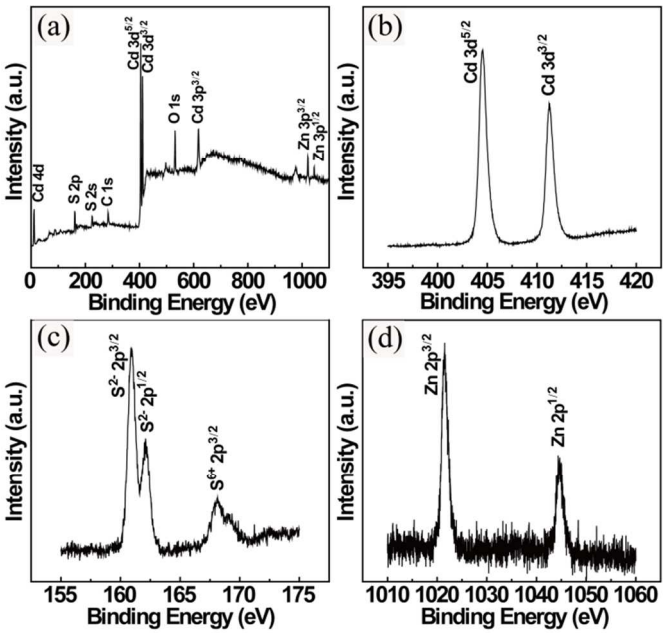

Fig. 2. (a) XPS spectrum of as-prepared Zn doped CdS nanobelts in the energy range of 0-1100eV. (b) High-resolution XPS for Cd $3d^{5/2}$ and Cd $3d^{3/2}$ peaks of Zn doped CdS nanobelts. (c) High-resolution XPS for S^{2-} $2p^{3/2}$, S^{2-} $2p^{1/2}$ and S^{6+} $2p^{3/2}$ peaks of Zn doped CdS nanobelts. (d) High-resolution XPS for Zn $2p^{3/2}$ and Zn $2p^{1/2}$ peaks of Zn doped CdS nanobelts.

The emissions of Zn doped CdS nanobelts are sensitive to the pumping laser power, as shown in the Fig. 3 (a). The ratio of integrated intensity of green emission and red emission (I_{green}/I_{red}) monotonically increase with the increase of pumping laser power. The corresponding PL spectra under different pumping power were shown in the inset of Fig. 3 (a), including the green band-edge emission and Zn-involved broad red trap-state emission. At higher power excitation, more photons are generated from the band-edge recombination, while at lower excitation, the red emission is dominant. Within the effective ratiometric changing range, each power of pumping laser yields a unique ratio of green emission and red emission intensity. The evolution of input power VS I_{green}/I_{red} are well fitted by the function $y = ax^b$, as shown with the red line in Fig. 3 (a), which is the basic calibration curve for the pumping power detect, where y is the ratio I_{green}/I_{red}, x is the pumping power, a is a fitting constant ($a = 4.80 * 10^{-4}$), $b = 2.69$ is a

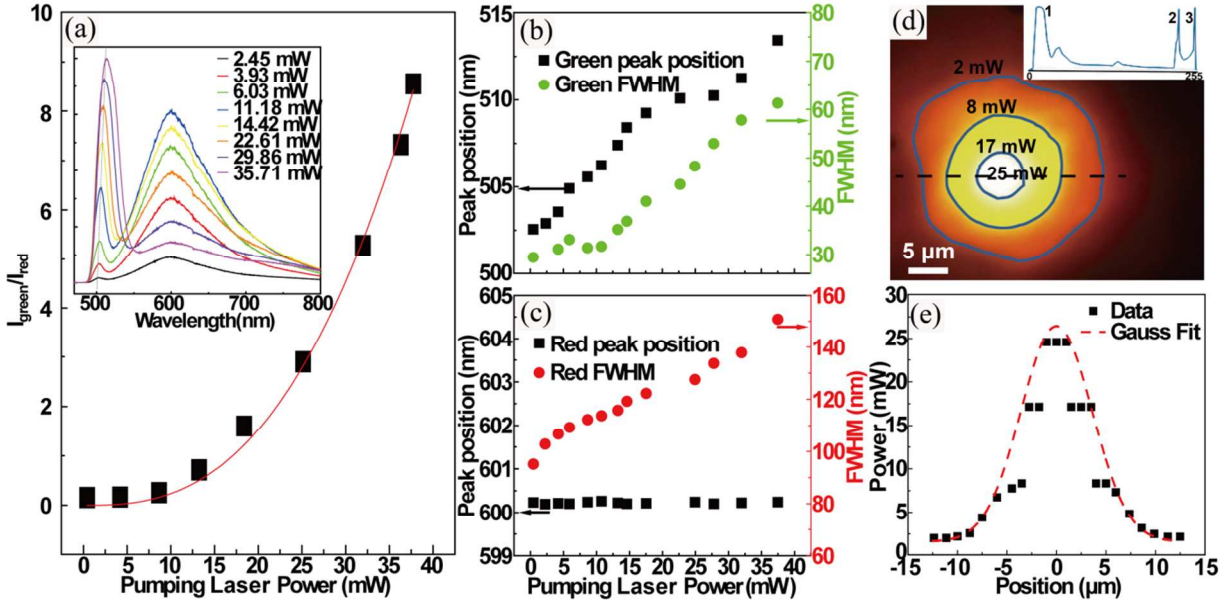

Fig. 3. (a) The intensity ratio of I_{green}/I_{red} as a function of pumping laser power. The data are well fitted by the function $y = ax^b$, marked as the red line, a is a fitting constant ($a = 4.8 * 10^{-4}$), $b = 2.69$ is a polynomial fitting index. The inset is the typical PL spectra of Zn doped CdS nanobelts with zinc-concentration at 2% under various pumping powers. (b) Peak position and FWHM of green emission as a function of pumping laser power. (c) Peak position and FWHM of red emission as a function of pumping laser power. (d) Real-color image of the laser spot excited on the on-chip Zn doped CdS nanobelts. At the center (white color part), the power is about 25 mW. The edges of the spot between the two different emitting colors are marked by the contours. The corresponding power values, 17 mW, 8 mW and 2 mW, are deduced by the PL intensity ratio and color. The inset is the distribution of color-density level. (e) Plot of the intensity profile of focal laser spot along the black dash line shown in Fig. 3 (d), marked as the black squares. The data are well fitted by the Gaussian curve, marked as the red dash line.

polynomial fitting index. Using this fitting function, the pending input laser power can be obtained by the PL ratio of I_{green}/I_{red} quantitatively. Furthermore, with the PL spectra under various pumping laser power, the green peak position is tuned from 503 nm to 514 nm with a relative red-shift about 11 nm (0.06 eV) as the increasing of excitation laser power from 2.62 mW to 37.49 mW, as shown in Fig. 3 (b). This red-shift is a characteristic of most Ⅱ-Ⅵ semiconductor nanobelts under the high pumping laser power, that is, the recombination from the free-excitons is dominant in the Zn doped CdS nanobelts at low pumping laser power; and then more free-excitons are generated and some of them can be ionized into free electrons and holes by the carrier-to-carrier scattering at higher pumping laser power,[21] which induces the redshift of green peak position.[22] Furthermore, the shallow bond states might come from the sulfide vacancies (V_S). Besides, the red peak position at ~600 nm has no obvious shift with laser power increase, as shown in Fig. 3 (c), which demonstrate that the red band originate from the Zn-related defect/surface related trap state emission.[21, 23] In addition, the full width at half maximum (FWHM) of green emission and red emission are both broaden with the pumping power increase, as shown in Fig. 3 (b) and Fig. 3 (c), respectively. These FWHM broadens are due to the more carries were generated and the potential fluctuations caused by higher pumping laser power.[21] Therefore, the PL properties of on-chip Zn doped CdS nanobelts can be tuned by the pumping power. Accordingly, the input laser power can be monitored by the monotonous change of emission intensity ratio of I_{green}/I_{red} from the on-chip Zn doped CdS nanobelts. The single-chip nanobelts materials can be used as the laser power monitors.

The detail profile of laser focal spot also can be measured by the on-chip Zn doped CdS nanobelts, as shown in Fig. 3 (d), a typical real-color PL image induced by a focused laser diode with the wavelength of 405 nm. At the center part (white color), the intensity of laser power is around 25 mW and the white light is formed due to CCD saturation. The intensity of laser spot is gradually lower away from the center of the laser spot, while the emitting color of Zn doped CdS nanobelts is changing from yellow-color to orange-yellow-color. Through the different color emitting image on the single-chip Zn doped CdS nanobelts, the intensity distribution of the excited laser spot can be detected. To clearly illuminate the distribution, the contour edges of different emitting colors are marked by the contours, as shown in Fig. 3 (d). The corresponding power values, 17 mW, 8 mW and 2 mW, were deduced by the PL intensity ratio and color. The inset of Fig. 3 (d) shows the distribution level of color gradation, the three peaks corresponds to the three bright color distributions, white, yellow and orange. The total laser focused spot and scanning region is clearly demonstrated by the color contour within 20 μm diameter effective range. For the CCD type laser profile display mode, it is hard to estimate the condensed laser focused spot profile due to the intense laser fluence damaging the CCD detector easily. To utilize the sensitivity of PL ratio of I_{green}/I_{red} on the pumping power value, the excited laser power can be deduced by the emitting color of Zn doped CdS nanobelts. Furthermore, the detail intensity distribution value of laser spot along the black dash line (shown in Fig. 3 (d)) is shown in Fig. 3 (e), as marked by the black squares. The intensities of focused pumping laser are deduced

from the corresponding the PL intensity ratio. These data of intensity are well fitted by the Gaussian curve, as marked by the red dash line in Fig. 3 (e). It is consistent to the distributions of commercial laser.[24] Using single-chip Zn doped CdS nanobelts, the distributions of the laser spot intensity distribution in micron region can be measured visually and intuitively, which has a potential application to detect and analyze the really effective laser focal range in many researches of nonlinear optical properties and femto-laser related micro/nano fabrication technique.

The laser power measurement and spot profile of input laser was measured using the setup, as shown in Fig. 4 (a). The laser beam was focused on the chip of Zn doped CdS nanobelts through a beamsplitter and an objective lens (X50), then the PL of the nanobelts were recorded in a spectrometer by the same beamsplitter and a mirror. Each pumping laser power yields a unique PL spectrum, according to the black reference curve of Fig. 4 (b), which is the same calibration curve shown in Fig. 3 (a) the real input pumping power were identified by the on-chip nanobelts, as shown in Fig. 4 (b). Five different-powers of laser were applied and the input power values were deduced by the I_{green}/I_{red} of 0.0082, 0.2876, 1.2843, 3.8149, 7.8046; and the corresponding laser power values are 2.87 mW, 10.78 mW, 18.8 mW, 28.18 mW and 36.77 mW, respectively, which were compared to the results measured by a commercial power meter (red circle dots) with the values are 2.62 mW, 10.48 mW, 20.71 mW, 27.26 mW and 37.49 mW, respectively. The root-mean-square error of the PL ratiometric method to the power meter measurement is about 5.37%. In addition, the typical real-color images of the on-chip nanobelts are excited by the pumping laser with 2.62 mW, 10.49 mW and 37.49 mW, which are shown in Fig. 4 (c) from left to right, respectively. The color in Fig. 4 (c) corresponds to the average power of the whole light spot. It is clearly shown that the color is tuned from orange-yellow to yellow and finally to green with the pumping power increase. The basic color changing with input laser provides us the basic reference standard to estimate the color-related laser spot profile, which provide an virtual way to estimate the different laser power roughly. Fig. 4 (d) shows the UV-visible absorption spectrum of the collective Zn doped CdS nanobelts, which reveals that the Zn doped CdS nanobelts can absorb the ultraviolet and up to blue light with the wavelength range less than 500 nm. However, these nanobelts hardly absorb the light with the wavelength longer than 500 nm. It demonstrates that the on-chip Zn doped CdS nanobelts can only detect the blue to ultraviolet light for the less absorption of yellow and red light. Therefore, the pumping laser power can be visually perceived by the emitting color, which is convenient on the application of nanoscale blue-violet laser power monitor.

To confirm the stability and effectiveness of this kind of nanostructure based detect elements on monitoring the laser power, more than two thousand cycles of input laser induced color switching between yellow-color emission and green-color emission have been real-timing recorded on the single-chip Zn doped CdS nanobelts, as shown in Fig. 4 (e). The x-axis is the color switching circles (in counts N) and the y-axis is the ratio of I_{green}/I_{red} from the minimum to the maximum. Besides, after the material preserved in dryer after 6 months and continuously irradiated during about 3 hours without any polymer covered on the chip surface, the laser power detection function of nanobelts-chip remains almost no change; and the intensity of luminescence is similar with previously results. The luminescence maintains around 650 Cd/m^2 with the pumping laser power of 35 mW. Observation of this extraordinary reversible and photoswitchable phenomenon is contributed to the ultra-photostability of the single-chip Zn doped CdS nanobelts, which is much better than the series of doped CdS nanocrystals that keep stable emission usually within several days.[25, 26] Moreover, the response and recovery time after laser excitation are determined by the lifetime of PL, the decay time of the band-edge and defect related emission is less than 1 ns and several nanosecond of Zn doped CdS nanoblets (see supporting information), respectively. This means that this kind of detector can be used on real-time laser monitor. Utilizing the nanostructure-based PL ratiometric method to monitor laser power opens a new way to fabricate power meter in micro/nanoscale.

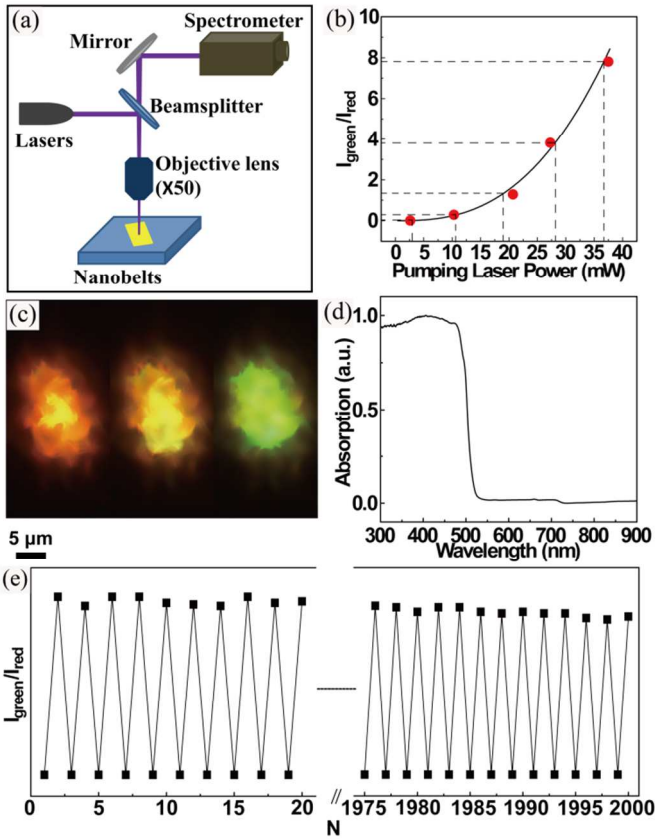

Fig. 4.(a) The diagram of set-up to detect the pumping laser power through the optical measurement. (b) The input laser power was obtained by the intensity ratio of I_{green}/I_{red} based on the standard reference curve (black curve from Fig. 3 (a)), contrasted to the power value of commercial power meter measurement (red circles). (c) Optical images of the collective Zn doped CdS nanobelts under a power of 2.62 mW, 10.49 mW and 37.49 mW from the left to the right. (d) The UV-visible absorption spectrum of the collective Zn doped CdS nanobelts. (e) The color switching cycles (in counts N) of the Zn doped CdS nanobelts under two pumping laser powers (2.62 and 37.49 mW).

Conclusions

In conclusion, we presented a new type of single-chip Zn-doped-CdS-nanobelt-based laser power detector, which show the input laser power and distribution visually and intuitively by the emission color change, exhibiting the potential applications on the laser power monitor and the analysis on the profile of laser focal spot in the micron region. Especially,

extraordinary stability and reversibility of the single-chip Zn doped CdS nanobelts confirm that this kind of nanostructure-based laser power detector have widely potential applications on ultraviolet and blue range laser power monitor to compose the complicatedly optical integrated circuits in micro/nanoscale.

Acknowledgements

This work was supported by the National Natural Science Foundation of China (No. 51002011) and the Basic Scientific Research Project of Beijing Institute of Technology

Notes and references

Beijing Key Lab of Nanophotonics and Ultrafine Optoelectronic Systems, School of Physics, Beijing Institute of Technology, Beijing 100081, China.
* Corresponding author. Tel.: +86 10 68918188; fax: +86 10 68918188.E-mail address: liuruibin8@gmail.com (R.B. Liu)
Electronic Supplementary Information (ESI) available: [details of any supplementary information available should be included here]. See DOI: 10.1039/b000000x/

1. S. Kodato, Y. Naito, K. Kuroda and S. Kodama, *Sensors and Actuators a-Physical*, 1991, **28**, 63-68.
2. C. S. Li, X. Cui and T. Yoshino, *Journal of Lightwave Technology*, 2003, **21**, 1328-1333.
3. O. Benson, *Nature*, 2011, **480**, 193-199.
4. J. Sun, E. Timurdogan, A. Yaacobi, E. S. Hosseini and M. R. Watts, *Nature*, 2013, **493**, 195-199.
5. J. Jie, W. Zhang, I. Bello, C.-S. Lee and S.-T. Lee, *Nano Today*, 2010, **5**, 313-336.
6. R. B. Liu, Z. A. Li, C. H. Zhang, X. X. Wang, M. A. Kamran, M. Farle and B. S. Zou, *Nano Lett.*, 2013, **13**, 2997-3001.
7. E. J. McLaurin, L. R. Bradshaw and D. R. Gamelin, *Chem. Mater.*, 2013, **25**, 1283-1292.
8. J. Beltran-Huarac, J. Wang, H. Tanaka, W. M. Jadwisienczak, B. R. Weiner and G. Morell, *J. Appl. Phys.*, 2013, **114**, -.
9. P. Shao, Q. Zhang, Y. Li and H. Wang, *J. Mater. Chem.*, 2011, **21**, 151-156.
10. O. Chen, D. E. Shelby, Y. Yang, J. Zhuang, T. Wang, C. Niu, N. Omenetto and Y. C. Cao, *Angew. Chem. Int. Ed.*, 2010, **49**, 10132-10135.
11. R. m. Beaulac, P. I. Archer, J. van Rijssel, A. Meijerink and D. R. Gamelin, *Nano Lett.*, 2008, **8**, 2949-2953.
12. N. S. Lee, G. Sun, L. Y. Lin, W. L. Neumann, J. N. Freskos, A. Karwa, J. J. Shieh, R. B. Dorshow and K. L. Wooley, *J. Mater. Chem.*, 2011, **21**, 14193-14202.
13. X. Sun, B. Liu and Y. Xu, *Analyst*, 2012, **137**, 1125-1129.
14. Y. Chen, C. Zhu, Z. Yang, J. Chen, Y. He, Y. Jiao, W. He, L. Qiu, J. Cen and Z. Guo, *Angew. Chem. Int. Ed.*, 2013, **52**, 1688-1691.
15. T.-Y. Sun, D.-Q. Zhang, X.-F. Yu, Y. Xiang, M. Luo, J.-H. Wang, G.-L. Tan, Q.-Q. Wang and P. K. Chu, *Nanoscale*, 2013, **5**, 1629-1637.
16. C. S. Li, T. Yoshino and X. Cui, in *Advanced Sensor Systems and Applications*, eds. Y. J. Rao, J. D. Jones, H. Naruse and R. I. Chen, 2002, pp. 1-8.
17. D.-b. Wang and X.-p. Liao, *Microsystem Technologies-Micro-and Nanosystems-Information Storage and Processing Systems*, 2011, **17**, 1343-1349.
18. K. Karki, M. Namboodiri, T. Z. Khan and A. Materny, *Appl. Phys. Lett.*, 2012, **100**.
19. H. Wang, Q. Zhang, J. Zhang, L. Li, Q. Zhang, S. Li, S. Zhang, J. Wu and Y. Tian, *Dyes and Pigments*, 2014, **102**, 263-272.
20. K. Heo, H. Lee, Y. Park, J. Park, H.-J. Lim, D. Yoon, C. Lee, M. Kim, H. Cheong, J. Park, J. Jian and S. Hong, *J. Mater. Chem.*, 2012, **22**, 2173-2179.
21. B. C. Cheng, Z. H. Han, H. J. Guo, S. Lin, Z. D. Zhang, Y. H. Xiao and S. J. Lei, *J. Appl. Phys.*, 2010, **108**.
22. R. B. Liu, Y. J. Chen, F. F. Wang, L. Cao, A. L. Pan, G. Z. Yang, T. H. Wang and B. S. Zou, *Physica E-Low-Dimensional Systems & Nanostructures*, 2007, **39**, 223-229.
23. S. Bhandari, R. Begum and A. Chattopadhyay, *Rsc Advances*, 2013, **3**, 2885-2888.
24. Y. Zhang, Y. Ning, Y. Wang, J. Cui, G. Liu, X. Zhang, Z. Wang, T. Li, L. Qin, Y. Sun, Y. Liu and L. Wang, *Optics Communications*, 2010, **283**, 2719-2723.
25. J. Tang, L. Brzozowski, D. A. R. Barkhouse, X. Wang, R. Debnath, R. Wolowiec, E. Palmiano, L. Levina, A. G. Pattantyus-Abraham, D. Jamakosmanovic and E. H. Sargent, *ACS Nano*, 2010, **4**, 869-878.
26. S. Xu, C. Wang, Z. Wang, H. Zhang, J. Yang, Q. Xu, H. Shao, R. Li, W. Lei and Y. Cui, *Nanotechnology*, 2011, **22**.